J. Fluid Mech. (1976), *vol.* 74, *part* 3, *pp.* 415–431
Printed in Great Britain

Free convection and the burning of a horizontal fuel surface

By J. F. CLARKE
Aerodynamics Division, Cranfield Institute of Technology, Bedford, England
AND N. RILEY
School of Mathematics and Physics, University of East Anglia, Norwich, England

(Received 24 July 1975)

The free-convective flow induced when a semi-infinite horizontal fuel surface burns in a quiescent oxidizing atmosphere is considered. For high values of the Grashof number the dominant feature of the flow is a boundary layer close to the surface within which there is a flame or intense reaction zone. An outer flow or fire-wind is induced by entrainment into this boundary layer. A simple experiment supports this overall picture of the flow.

1. Introduction

In this paper we consider the flow over the *horizontal* surface $-\infty < x < \infty$, $y = 0$ which is induced when the fuel surface $x > 0$, $y = 0$ burns in an oxidizing atmosphere. The surface $x < 0$, $y = 0$ is supposed impermeable and chemically inert.

Stewartson (1958) showed that when the upper surface of a semi-infinite horizontal solid surface is heated induced pressure gradients lead to the development of a boundary-layer flow over the upper surface, commencing at the leading edge. Stewartson assumed the fluid to be a Boussinesq fluid and therefore accounted for density variations only in the buoyancy term. With the same assumption Rotem & Claassen (1969) extended Stewartson's solutions and, using a colour schlieren technique, provided qualitative experimental confirmation of the existence of such a flow. Jones (1973) showed that if the plate is inclined downwards slightly then the initial flow development is as for the horizontal case but that the flow eventually separates. Clarke & Riley (1975, henceforth referred to as I) considered the prototype problem of Stewartson but allowed for density changes and temperature-dependent viscosity and thermal conductivity. They also allowed the heated surface to be permeable and considered the effects of blowing upon the flow.

In the present work the horizontal surface $-\infty < x < \infty, y = 0$ is such that for $x < 0$ it is impermeable and inert whilst for $x > 0$ it is a fuel surface, either solid or liquid. The fuel in $x > 0$ is allowed to evaporate from the surface and burn in the oxidizing atmosphere $y > 0$. The analysis in I, which includes the effects of transpiration from the surface, models the evaporative nature of the

fuel surface. In this combustion problem a flame-sheet model is adopted so that there is a thin intense reaction zone, not coincident with the fuel surface, in which chemical energy is liberated. Although the fluid is therefore heated internally, rather than from the surface, the same mechanisms as induce a pressure gradient in the inert case are responsible for the flow under consideration. The Boussinesq approximation is not appropriate here and, as in I, we use Howarth's transformation, which allows one to take account of density changes, in order to describe the boundary-layer flow.

Free convection associated with the burning of a vertical or inclined semi-infinite plate has been considered by Kim, de Ris & Kroesser (1971). In that particular configuration buoyancy effects are *directly* responsible for the fluid motion. Like Kim *et al.* we adopt a one-step irreversible chemical reaction to describe the chemical kinetics and we assume that the Lewis number is unity so that we may introduce the so-called Shvab–Zeldovich variables. We also assume that the Grashof number is large, which allows us to adopt a perturbation approach in our solution of the governing equations.

In §2 the governing equations are derived under the assumptions outlined above. In §3 advantage is taken of the high Grashof number and the leading terms in each of outer and inner, or boundary-layer, regions are derived. The results are discussed in §4 with particular attention given to the flame-sheet location, surface heat and mass transfer rates and surface shear stress. Also, the phenomenon of 'surface combustion' is briefly discussed. The flow in the outer region is induced by the sink-like effect of the boundary layer. Thus the boundary layer entrains fluid from the ambient oxidizing atmosphere, and it is this which enables the combustion process to be maintained. This outer flow models the 'fire-wind' which is observed to blow over the perimeter of a fire of finite extent. Smith, Morton & Leslie (1975) point out that conventional fire-plume models fail to provide an adequate explanation for the fire-wind. They consider a chemically inert situation in which a finite strip in the horizontal boundary $-\infty < x < \infty, y = 0$ is maintained at a higher temperature than the ambient, and solve the Navier–Stokes equations numerically. They conclude that the fire-wind is associated with the dynamic pressure field, which produces a strong coupling between the fire zone and its environment. This view is confirmed by our work, at least in so far as the motion arises from induced pressure gradients within the boundary layer due to density changes brought about by heat release in the combustion zone.

In §5 we describe a simple experiment which supports the results that we have obtained. Solid combustible material of finite extent is embedded in a horizontal surface and bounded laterally to simulate a plane flow. A boundary layer develops from each edge of the combustible material. Although these boundary layers eventually interact to form a buoyant vertical plume, the flame sheet in the neighbourhood of a leading edge may be expected to behave as predicted analytically for the semi-infinite geometry. Schlieren pictures substantiate this expectation both qualitatively and, to some degree, quantitatively too.

2. The governing equations

A one-step, irreversible chemical reaction scheme is adopted in which

$$\nu_X X + \nu_F F \rightarrow \nu_P P, \tag{1}$$

where X, F and P denote oxidant, fuel and product species respectively. The quantities ν_α ($\alpha = X, F, P$) in (1) are the stoichiometric integers. The equations of motion for steady flow of a compressible fluid, in the small Mach number limit, may be written in dimensionless form as follows:

$$\partial(\rho u_k)/\partial x_k = 0, \tag{2}$$

$$\rho u_k \frac{\partial u_j}{\partial x_k} + \frac{\partial p}{\partial x_j} = \epsilon^{\frac{4}{3}} \frac{\partial}{\partial x_k}\left\{\frac{\partial u_k}{\partial x_j} + \frac{\partial u_j}{\partial x_k} - \frac{2}{3}\frac{\partial u_k}{\partial x_k}\right\} + \epsilon^{-\frac{2}{3}}(\rho - 1)\, n_j, \quad n_j = (0, -1), \tag{3}$$

$$\rho u_k \frac{\partial \beta_\alpha}{\partial x_k} = \frac{\epsilon^{\frac{4}{3}}}{\sigma}\frac{\partial}{\partial x_k}\left\{\lambda \frac{\partial \beta_\alpha}{\partial x_k}\right\}, \quad \alpha = X, F, \tag{4a}$$

where

$$\beta_F = \theta + Q\gamma_F, \quad \beta_X = \theta + Q(\gamma_X - \gamma_{X_\infty}), \tag{4b}$$

$$\rho(1+\theta) = 1. \tag{5}$$

In these equations $(x_1, x_2) \equiv (x, y)$ are dimensionless co-ordinates based on a length L, the dimensionless velocity components $(u_1, u_2) \equiv (u, v)$ are referred to the velocity $U_r = \nu_\infty^{\frac{1}{3}} g^{\frac{2}{3}} L^{\frac{1}{3}}$, and the pressure p is referred to $\rho_\infty U_r^2$, where a subscript ∞ denotes a value in the ambient atmosphere. The scales for the dimensionless density ρ, coefficient of viscosity μ, thermal conductivity λ and temperature θ are chosen as ρ_∞, μ_∞, λ_∞ and T_∞, where it is convenient to define θ such that $\theta \equiv 0$ in the ambient atmosphere. The quantities γ_α ($\alpha = X, F$) are the stoichiometrically adjusted mass fractions related to the species mass fractions c_α by $\gamma_\alpha = c_\alpha / \nu_\alpha W_\alpha$, where W_α represents the molecular weight. We define

$$Q = (\nu_X W_X + \nu_F W_F) H,$$

where $-H$ is the dimensionless energy of formation of the product species P, so that $Q > 0$. We note that all dimensionless energies are referred to $C_p T_\infty$, where C_p is the coefficient of specific heat at constant pressure, assumed the same for all species. The parameter ϵ, which characterizes the flow under consideration, is related to the Grashof number $Gr = L^3 g/\nu_\infty^2$ by $\epsilon = Gr^{-\frac{1}{4}}$ and throughout we assume $Gr \gg 1$. The Prandtl number σ is assumed to be constant as is the Schmidt number; the Lewis number is taken as unity.

Equations (2) and (3) are the continuity and momentum equations respectively and we note that in (3) we have assumed that there is no contribution to the buoyancy force from changes in composition. Equations (4) are the Shvab–Zeldovich forms for energy and species conservation. The advantages of the Shvab–Zeldovich formulation for the coupling functions β_α are that the energy and mass source terms associated with the chemical reaction do not appear explicitly. Equation (5) is the equation of state. If, in (4), we set $Q \equiv 0$ then (2)–(5) are as for the inert-gas case, which has been discussed extensively in I, although it should be noted that in I the choice of the typical length L differs slightly from that adopted here.

Since the coupling functions which satisfy (4*a*) involve a combination of the temperature and mass fractions further information is necessary before the system of equations, together with boundary conditions which are to be prescribed, is determinate. Here we adopt the assumption that the chemical time associated with the irreversible reaction (1) is zero. This, the so-called Burke–Schumann limit, results in a flame-sheet model in which the intense chemical reaction is confined to the sheet $y = y_s(x)$, whose location is unknown *a priori*. Very small chemical times are realized in practice and for the detailed structure of this flame zone reference may be made to Clarke (1975). It is sufficient for our purposes to note that

$$\left.\begin{aligned} c_F &\equiv 0, \quad y > y_s(x), \\ c_X &\equiv 0, \quad y < y_s(x). \end{aligned}\right\} \tag{6}$$

We remark that although the mass fractions and temperature are continuous at the flame sheet their first derivatives are not. However the coupling functions β_α, which satisfy (4*a*), *are* continuous with continuous first and second derivatives.

It is the heat released in the flame zone which is directly responsible for the induced horizontal pressure gradient, which in turn maintains the flow under consideration.

Consider now the boundary conditions which are to be satisfied. As we go away from the boundary the ambient conditions must ultimately be realized, thus

$$u, v, p, \theta, \beta_\alpha (\alpha = X, F) \to 0 \quad \text{as} \quad (x^2 + y^2)^{\frac{1}{2}} \to \infty, \quad y \neq 0. \tag{7}$$

For $x < 0, y = 0$ we have an impermeable, chemically inert, insulating surface and so

$$u, v, \frac{\partial \theta}{\partial y}, \frac{\partial \beta_\alpha}{\partial y} (\alpha = X, F) = 0 \quad \text{for} \quad x < 0, \quad y = 0. \tag{8}$$

The boundary conditions on the evaporating fuel surface $x > 0, y = 0$ require a more careful consideration. Whether it is a solid surface or the surface of a liquid-fuel pool we assume that it is a no-slip surface, for in the latter case we may anticipate that in this combustion situation the surface will become contaminated and therefore behave like a rigid surface. This means of course that we are neglecting any induced fluid motion within a liquid-fuel pool. Thus

$$u = 0 \quad \text{for} \quad x > 0, \quad y = 0. \tag{9}$$

The transpiration velocity from the fuel surface is not prescribed but is to be determined; we write the dimensionless rate of surface mass transfer as $\dot{m} = \rho v|_{y=0}$. We assume that the surface maintains its constant vapourization temperature to give

$$\theta = \Delta \quad \text{for} \quad x > 0, \quad y = 0. \tag{10}$$

The dimensionless adiabatic evaporation condition at the surface, which states that all the energy transfer goes into liberating fuel vapour, yields

$$\epsilon^{\frac{1}{2}} \frac{\lambda}{\sigma} \frac{\partial \theta}{\partial y} = \dot{m} \mathscr{L} \quad \text{for} \quad x > 0, \quad y = 0, \tag{11}$$

where $\mathscr{L}$ is the dimensionless latent heat. Finally we have the condition that only fuel and inert gases emerge from the surface. This condition gives

$$\epsilon^{\frac{1}{2}}\frac{\lambda}{\sigma}\frac{\partial \gamma_F}{\partial y} = \dot{m}(\gamma_F - \gamma_{FT}) \quad \text{for} \quad x > 0, \quad y = 0, \tag{12}$$

where it should be noted that c_{FT} is the mass fraction of fuel in the transferred gas (see Kim *et al.* 1971).

Equations (2)–(6) together with the boundary conditions (7)–(12) now give us a determinate system. However, before discussing solutions we consider further simplifying implications of the above.

From (4*b*), (6) and (11) we have

$$\epsilon^{\frac{1}{2}}\frac{\lambda}{\sigma}\frac{\partial \beta_X}{\partial y}\bigg|_{y=0} = \dot{m}\mathscr{L}, \tag{13}$$

and use of (4*b*) and (10) in (12) gives

$$\epsilon^{\frac{1}{2}}\frac{\lambda}{\sigma}\left\{\frac{\partial \beta_F}{\partial y} - \frac{\partial \theta}{\partial y}\right\}_{y=0} = \dot{m}\{\beta_F|_{y=0} - \Delta - Q\gamma_{FT}\}. \tag{14}$$

We may then combine (13) and (14) such that

$$\frac{\partial \beta_F}{\partial y}\bigg|_{y=0} = \left\{1 - \frac{\Delta}{\mathscr{L}} - \frac{Q}{\mathscr{L}}\gamma_{FT} + \frac{\beta_F|_{y=0}}{\mathscr{L}}\right\}\frac{\partial \beta_X}{\partial y}\bigg|_{y=0}. \tag{15}$$

We note in (15) that Δ, Q, γ_{FT} and $\mathscr{L}$ are all constants; if we make the further assumption $\beta_F|_{y=0} = \text{constant}$, an assumption which will be seen to be justified *a posteriori*, then (15) shows that $[\partial\beta_F/\partial y]_{y=0} \propto [\partial\beta_X/\partial y]_{y=0}$. This result, together with (4*a*) and (7), shows that $\beta_X \propto \beta_F$, and it is convenient to introduce the function $\beta = \beta(x, y)$ such that

$$\beta_\alpha = -A_\alpha \beta, \quad \alpha = X, F, \tag{16}$$

where A_α is constant. Like β_α the quantity β is continuous with continuous first and second derivatives and satisfies

$$\rho u_k \frac{\partial \beta}{\partial x_k} = \frac{\epsilon^{\frac{1}{2}}}{\sigma}\frac{\partial}{\partial x_k}\left\{\lambda\frac{\partial \beta}{\partial x_k}\right\}. \tag{17}$$

The constants A_α may be expressed in terms of the other physical constants as follows. If we define

$$\beta(x, 0) = 1, \tag{18}$$

then (16) gives, using (4*b*) and (10),

$$A_X = -\beta_X(x, 0) = Q\gamma_{X_\infty} - \Delta, \tag{19}$$

and (15) gives

$$A_F = \{\mathscr{L} - Q\gamma_{FT} - \Delta\}\{A_X/(A_X + \mathscr{L})\}. \tag{20}$$

The values of the modified coupling function β and temperature θ at the flame sheet can also be expressed in terms of the other physical constants. Thus if a

subscript s is used to denote a quantity evaluated at the flame sheet, we deduce from (6) that $\gamma_{X_s} = \gamma_{F_s} = 0$ and from (4b) we have

$$\beta_{Fs} = \theta_s = \beta_{X_s} + Q\gamma_{X_\infty}, \tag{21}$$

from which we may deduce, using (16), (19) and (20),

$$\left.\begin{aligned} \beta_s &= \left(\frac{\gamma_{X_\infty}}{\gamma_{X_\infty}+\gamma_{FT}}\right)\left(\frac{\mathscr{L}+A_X}{A_X}\right), \\ \text{and} \qquad \theta_s &= \left(\frac{\gamma_{X_\infty}}{\gamma_{X_\infty}+\gamma_{FT}}\right)(Q\gamma_{FT}+\Delta-\mathscr{L}). \end{aligned}\right\} \tag{22}$$

It also proves convenient to express A_X and A_F in terms of β_s and θ_s. From (20) and (22) we have at once that

$$A_F = -\theta_s/\beta_s. \tag{23}$$

Now, from (16) and (21) we have $\theta_s = -A_X\beta_s + Q\gamma_{X_\infty}$, so that

$$A_X = (Q\gamma_{X_\infty} - \theta_s)/\beta_s, \tag{24}$$

and combining (19) with (24) gives

$$Q\gamma_{X_\infty} = (\theta_s - \beta_s\Delta)/(1-\beta_s), \tag{25}$$

so that

$$A_X = (\theta_s - \Delta)/(1-\beta_s). \tag{26}$$

In summary, with

$$\beta_\alpha = -A_\alpha\beta, \quad \alpha = X, F, \tag{27}$$

and the temperature θ given from (4b) and (6) as

$$\theta = \begin{cases} -A_F\beta & \text{for} \quad y > y_s(x), \\ -A_X\beta + Q\gamma_{X_\infty} & \text{for} \quad y < y_s(x), \end{cases} \tag{28}$$

we have to solve (2), (3), (5) and (17) subject to the boundary conditions (7)–(9), (13) and (18). The solution procedure is described in § 3 and the results discussed in § 4.

3. The solution procedure

In the high Grashof number situations which we envisage, we are able to take advantage of the presence of the small parameter ϵ in our governing equations. Thus we develop asymptotic solutions, formally valid as $\epsilon \to 0$, in both an outer and an inner or boundary-layer region. The approach closely parallels that adopted in I for the inert case.

To first order (17) shows that β must be constant on any streamline provided $|u_j| > \text{ord}(\epsilon^{\frac{1}{2}})$. Thus we may assume, from the conditions (7), that $\beta = o(1)$ everywhere in this outer region. The singular perturbation character of the problem is immediately obvious since this outer solution cannot satisfy the condition (18). The situation is similar for the velocity field because, if we assume that $\beta = o(\epsilon^{\frac{1}{2}})$ in the outer region, an assumption which we justify below, then (3) show that the vorticity is constant, and by virtue of (7), zero on each streamline in the outer region. This in turn implies that there is no $O(1)$ motion in the

outer region. As in I we shall find that ord (1) > $|u_j|$ > ord ($\epsilon^{\frac{1}{5}}$) in this outer region and hence these deductions are valid.

The above results are consistent with the notion that the flow under consideration is driven within the boundary layer, or inner region, by the effects of internal heating. We shall see that the disturbance to the ambient conditions in the outer region is brought about by entrainment into the boundary layer exactly as in the inert case I.

Consider now the flow in the inner, or boundary-layer region. As in I we define inner variables as follows:

$$\left.\begin{aligned} &x = x, \quad Y = \epsilon^{-\frac{2}{5}} y, \quad f = f(x,y,\epsilon) = \epsilon^{i} \mathscr{F}(x, Y, \epsilon), \\ \text{where} \quad &i = 0 \quad \text{for} \quad f = u, p, \theta, \beta, \rho, \quad i = \tfrac{2}{5} \quad \text{for} \quad f = v, \psi. \end{aligned}\right\} \tag{29}$$

In (29), $\mathscr{F}$ is equal to U, V, P, R, B, Θ or Ψ when f is equal to u, v, p, ρ, β, θ or ψ respectively. The stream functions Ψ and ψ in the inner and outer regions respectively are defined such that

$$\left.\begin{aligned} \rho u &= \partial\psi/\partial y = \partial\Psi/\partial Y = RU, \\ \rho v &= -\partial\psi/\partial x = -\epsilon^{\frac{2}{5}} \partial\Psi/\partial x = \epsilon^{\frac{2}{5}} RV, \end{aligned}\right\} \tag{30}$$

so that the continuity equation (2) is automatically satisfied.

In terms of these variables (3) and (17) become, ignoring terms which are $o(1)$ in ϵ,

$$\frac{\partial(U,\Psi)}{\partial(x,Y)} + \frac{\partial P}{\partial x} = \frac{\partial}{\partial Y}\left(\mu \frac{\partial U}{\partial Y}\right), \tag{31a}$$

$$\partial P/\partial Y = 1 - R = R\Theta, \tag{31b}$$

$$\frac{\partial(B,\Psi)}{\partial(x,Y)} = \frac{1}{\sigma}\frac{\partial}{\partial Y}\left(\lambda \frac{\partial B}{\partial Y}\right), \tag{31c}$$

where in (31b) the equation of state (5) has been employed. As we have emphasized earlier it is unrealistic in this combustion situation to make the Boussinesq approximation, in which the fluid properties are assumed to be constant, with density variations accounted for only in the buoyancy term in (3). Without this approximation we may still simplify the inner equations (31) by introducing the Howarth transformation from variables (x, Y) to (X, Z), where

$$\left.\begin{aligned} &x = X, \\ &Z = \int_0^Y R(x,s)\,ds = \int_0^Y \left\{1 - \frac{\partial P(x,s)}{\partial s}\right\} ds = Y - P(x,Y) + P(x,0). \end{aligned}\right\} \tag{32}$$

Thus

$$U = \frac{\partial\Psi}{\partial Z}; \quad \frac{\partial(A,\Psi)}{\partial(x,Y)} = R\frac{\partial(A,\Psi)}{\partial(X,Z)}, \quad A = U, B, \tag{33}$$

and

$$\frac{\partial P(x,Y)}{\partial x} = \frac{\partial P(X,Z)}{\partial X} + \frac{\partial P(X,Z)}{\partial Z}\left\{-\frac{\partial P(x,Y)}{\partial x} + \frac{\partial P_0}{\partial x}\right\}, \tag{34}$$

where $P_0 = P(x, 0)$. If we also make the assumption that the viscosity and conductivity are proportional to the temperature, so that, from (5),

$$\rho\mu = \rho\lambda = 1, \tag{35}$$

we have as the equations to be solved in the inner or boundary-layer region, from (28), (31) and (33)–(35),

$$\frac{\partial \Psi}{\partial Z}\frac{\partial^2 \Psi}{\partial X \partial Z} - \frac{\partial \Psi}{\partial X}\frac{\partial^2 \Psi}{\partial Z^2} + \frac{\partial P}{\partial X} + \Theta \frac{\partial P_0}{\partial X} = \frac{\partial^3 \Psi}{\partial Z^3}, \tag{36a}$$

$$\partial P/\partial Z = \Theta, \tag{36b}$$

$$\frac{\partial \Psi}{\partial Z}\frac{\partial B}{\partial X} - \frac{\partial \Psi}{\partial X}\frac{\partial B}{\partial Z} = \frac{1}{\sigma}\frac{\partial^2 B}{\partial Z^2}, \tag{36c}$$

$$\Theta = \begin{cases} -A_F B & \text{in} \quad Z > Z_s(X), \\ -A_X B + Q\gamma_{X_\infty} & \text{in} \quad Z < Z_s(X), \end{cases} \tag{36d}$$

with the Shvab–Zeldovich coupling functions subsequently determined from (27) and (29). The boundary conditions which have to be satisfied are determined, as $Z \to \infty$, by matching with the trivial solution in the outer region, so that

$$B, P, \partial \Psi/\partial Z \to 0 \quad \text{as} \quad Z \to \infty, \tag{37}$$

and at the fuel surface, from (9), (13) and (19),

$$\frac{\partial \Psi}{\partial Z} = 0, \quad \frac{\partial B}{\partial Z} = \frac{\mathscr{L}\sigma}{A_X}\frac{\partial \Psi}{\partial X}, \quad B = 1 \quad \text{at} \quad Z = 0, \tag{38a–c}$$

where in (38*b*) we have used $\rho v|_{y=0} = -\epsilon^{\frac{3}{2}}[\partial \Psi/\partial X]_{Z=0} = \dot{m}$.

As for the inert case, discussed in I, the boundary-layer equations (36) admit a similarity solution, for which we write

$$\left.\begin{aligned} &\Psi = \theta_s^{\frac{1}{5}} X^{\frac{3}{5}} F(\eta), \quad P = \theta_s^{\frac{4}{5}} X^{\frac{2}{5}} G(\eta), \\ &\Theta = \theta_s G'(\eta), \quad B = J(\eta), \\ &\eta = \theta_s^{\frac{1}{5}} Z / X^{\frac{2}{5}}. \end{aligned}\right\} \tag{39}$$

where

In terms of these new variables (36) become, using (23) and (26),

$$5F''' + 3FF'' - F'^2 - 2\{G - (\eta - \theta_s G(0))\, G'\} = 0, \tag{40}$$

$$G' = \begin{cases} J/\beta_s, & \eta > \eta_s, \\ \dfrac{1-J}{1-\beta_s} + \delta\left(\dfrac{J-\beta_s}{1-\beta_s}\right), & \eta < \eta_s, \end{cases} \tag{41}$$

$$5J'' + 3\sigma F J' = 0, \tag{42}$$

where a prime in these equations denotes differentiation with respect to η, and we have written $\delta = \Delta/\theta_s$. The boundary conditions (37) show that

$$J, G, F' \to 0 \quad \text{as} \quad \eta \to \infty. \tag{43a–c}$$

The boundary conditions (38) at $Z = 0$ now become, in terms of the similarity variables (39),

$$F'(0) = 0, \quad J'(0) = \frac{3}{5}\frac{\sigma \mathscr{L}}{\theta_s}\left(\frac{1-\beta_s}{1-\delta}\right) F(0), \quad J(0) = 1, \tag{44a–c}$$

and we note that the flame-sheet location is determined from

$$G'(\eta_s) = 1. \tag{45}$$

It has been found convenient when integrating the above equations numerically to eliminate the variable J. Thus, from (41) and (42), G satisfies

$$5G''' + 3\sigma FG'' = 0, \tag{46}$$

and at the wall $\eta = 0$, (44b, c) become

$$G''(0) = -\frac{3}{5}\frac{\sigma\mathscr{L}}{\theta_s}F(0), \quad G'(0) = \delta, \tag{47a, b}$$

whilst it is also required from (41) and (43a) that

$$G' \to 0 \quad \text{as} \quad \eta \to \infty. \tag{48}$$

It should be noted that, although

$$F, F', F'', G, G' (= 1) \quad \text{are continuous at} \quad \eta = \eta_s, \tag{49}$$

G'' is not continuous. The jump in G'' at $\eta = \eta_s$ may be calculated from (41) as

$$\frac{G''_+}{G''_-} = \frac{1-\beta_s}{\beta_s(\delta-1)}, \tag{50}$$

where the subscripts $\pm$ refer to $\eta = \eta_s \pm 0$ respectively.

The numerical method adopted to solve (40) and (46) subject to (43b, c), (44a) and (47a, b)–(50) is similar to that adopted for the inert-gas case in I, where it is described in more detail. Briefly, the range $0 \leqslant \eta \leqslant \eta_\infty$, where η_∞ is a finite quantity which is chosen to be sufficiently large to represent the outer edge of the boundary layer $\eta = \infty$, is divided into the two zones $\eta \gtrless \eta_s$. In each zone a Newton iteration procedure is adopted so that quasi-linearized forms of (40) and(46) are to be integrated. In each zone each dependent variable is represented by a finite Chebychev series as

$$\mathscr{H}(z) = \sum_{j=1}^{N} a_j T_{j-1}(z) \quad (\mathscr{H} = F, G), \tag{51}$$

where

$$z = \begin{cases} (2\eta - \eta_s)/\eta_s, & \eta < \eta_s, \\ 2(\eta - \eta_s)/L - 1, & \eta > \eta_s, \end{cases} \tag{52}$$

where $L = \eta_\infty - \eta_s$, so that $-1 \leqslant z \leqslant 1$ in each zone. The $4N$ coefficients of the type a_j in (51), which are required to define the solution in the Chebychev representation, are determined by satisfying the differential equations, linearized as indicated above, in each of $\eta \gtrless \eta_s$ at the $N-3$ points

$$z_m = \cos\{(m-1)\pi/(N-4)\}, \quad m = 1, \ldots, N-3. \tag{53}$$

This gives $4N-12$ equations for the $4N$ unknowns. The conditions (43b, c), (44a) and (47a, b)–(50) give a further 12 equations. The $4N$ unknown coefficients are thus determined by solving the $4N$ equations so derived and the iterative process proceeds as in I. The results of this numerical investigation are discussed in the next section.

Before we go on to examine the effects of the boundary-layer flow upon the solution in the outer region we observe that in this combustion problem we might expect the flame-sheet temperature θ_s to be large. We now discuss such a limiting situation.

The case we consider, formally in the limit $\theta_s \to \infty$, is that in which $\theta_s/\mathscr{L}$ remains finite, since in many cases the quantities $\mathscr{L}$ and θ_s are of comparable magnitude. If we define new variables in this limit as

$$\tilde{\phi} = \theta_s^{-\frac{1}{5}} F, \quad \tilde{\psi} = \theta_s^{\frac{1}{5}} G, \quad \xi = \theta_s^{\frac{1}{5}} \eta \quad \text{and write} \quad \mathscr{L} = \theta_s \mathscr{L}_s, \tag{54}$$

then (40) and (46) become

$$\left.\begin{aligned} 5\tilde{\phi}''' + 3\tilde{\phi}\tilde{\phi}'' - \tilde{\phi}'^2 - 2\tilde{\psi}(0)\,\tilde{\psi}' = 0, \\ 5\tilde{\psi}''' + 3\sigma\tilde{\phi}\tilde{\psi}'' = 0, \end{aligned}\right\} \tag{55}$$

where a prime now denotes differentiation with respect to ξ. The boundary conditions under which (55) have to be solved, again in the separate zones $\xi \gtrless \xi_s$, may be inferred from (43*b*, *c*), (44*a*) and (47*a*, *b*)–(50) by simply replacing F by $\tilde{\phi}$, G by $\tilde{\psi}$ and $\mathscr{L}$ by $\theta_s \mathscr{L}_s$ provided that we retain, as is reasonable, δ as a finite quantity in this limit. The method of solution of these modified equations (55) is exactly that which has been adopted for finite θ_s and the results are discussed in the next section.

We finally consider in this section the flow in the outer region, which has been shown to be quiescent and isothermal to first order. Now provided that the velocities in the outer region despite being $o(1)$ are nevertheless larger than $O(\epsilon^{\frac{1}{5}})$, and we show below that they are, we see that the leading term in the asymptotic solution of (17), regardless of its algebraic order in terms of the small parameter ϵ, must be such that it is constant along the streamlines of the outer flow. If these streamlines originate at infinity, and we shall show this to be the case, then to all orders $\beta = 0$ in the outer region. This justifies the assumption $\beta = o(\epsilon^{\frac{2}{5}})$ made in §2.

Consider next the velocity field. We see from (29) and (39), since $F(\infty) \neq 0$, that

$$\psi(x, 0) = \left\{\begin{aligned} &\epsilon^{\frac{2}{5}}\theta_s^{\frac{1}{5}} x^{\frac{3}{5}} F(\infty), \quad x > 0, \\ &0, \quad x < 0, \end{aligned}\right\} \tag{56}$$

is the appropriate asymptotic matching condition between the outer and inner solutions. Thus in the outer region we see from (56) that the velocity components are $O(\epsilon^{\frac{2}{5}})$. We may then infer, from (3), that along the streamlines of the outer flow the vorticity to this order is constant and therefore equal to zero if the streamlines originate at infinity. For this two-dimensional flow, therefore, we have $\nabla^2\psi = 0$ to this order and if we write $\psi = \epsilon^{\frac{2}{5}}\theta_s^{\frac{1}{5}} F(\infty)\,\psi_0$ the problem for ψ_0 is

$$\left.\begin{aligned} &\nabla^2\psi_0 = 0, \\ &\psi_0 = \begin{cases} 0, & x < 0, \quad y = 0, \\ x^{\frac{3}{5}}, & x > 0, \quad y = 0, \end{cases} \\ &\nabla\psi_0 \to 0 \quad \text{as} \quad (x^2+y^2)^{\frac{1}{2}} \to \infty, \quad y \neq 0. \end{aligned}\right\} \tag{57}$$

The solution for ψ_0 is

$$\psi_0 = r^{\frac{3}{5}} \sin\{\tfrac{3}{5}(\pi - \phi)\}/\sin\tfrac{3}{5}\pi, \quad \text{where} \quad r^2 = x^2+y^2, \quad \phi = \tan^{-1}(y/x). \tag{58}$$

This solution (58) for the outer flow gives, in turn, a non-zero component of velocity, $O(\epsilon^{\frac{2}{5}})$, parallel to the surface $y = 0$ which will be accommodated by the next term of the inner solution. We do not pursue the solution in the inner region to this order; some discussion of the inert flow case can be found in I.

4. Results

We consider first the results which have been obtained for the boundary-layer flow by numerically integrating (40) and (46) subject to the boundary conditions (43*b*, *c*), (44*a*), (47*a*, *b*) and (48). The technique which has been employed, as already indicated in §3, involves the division of the boundary layer into the two zones $\eta \gtrless \eta_s$. In each of these zones the dependent variables are represented by finite Chebychev series involving, in all, $4N$ unknown coefficients. These are determined by satisfying the differential equations, suitably linearized, at the points z_m in (53) in each zone, together with the boundary conditions and the conditions (49) and (50), which link the solution in each zone across $\eta = \eta_s$. In all the calculations carried out we chose $N = 20$, and the outer edge of the boundary layer was approximated by $\eta_\infty = 16$. It was found in practice that each of these values is sufficiently large to ensure four decimal place accuracy in the solutions. In the solution procedure adopted the boundary condition (47*a*) was not used directly. It was found to be convenient to specify $F(0)$. The flame-sheet location η_s must also be specified before the equations can be integrated. For each value of $\mathscr{L}$ the correct values of $F(0)$ and η_s were determined by linear interpolation between successive 'solutions' until the conditions (45) and (47*a*) were satisfied.

No fewer than five independent parameters characterize the boundary-layer solution. In our calculations we have maintained four of these at fixed values which we believe are representative of the combustion situations under consideration. Thus we choose $\sigma = 0{\cdot}72$, $\beta_s = 0{\cdot}5$, $\theta_s = 6{\cdot}0$ and $\delta = 0{\cdot}25$; we have allowed the latent heat $\mathscr{L}$ to vary in order that we may model the different materials from which the combustible surface $x > 0, y = 0$ may be formed. The important parameters which emerge from the calculations are the flame-sheet location η_s, the mass and heat transfer rates together with the shear stress at the fuel surface. We note, using (39), that

$$\left.\begin{aligned} F(0) &= -\tfrac{5}{3}\epsilon^{-\frac{2}{5}}\theta_s^{-\frac{1}{5}}x^{-\frac{3}{5}}\dot{m}, \\ G''(0) &= (1+\Delta)\,\epsilon^{\frac{2}{5}}\theta_s^{-\frac{2}{5}}x^{\frac{2}{5}}[\partial\theta/\partial y]_{y=0}, \\ F''(0) &= (1+\Delta)\,\epsilon^{\frac{2}{5}}\theta_s^{-\frac{3}{5}}x^{\frac{1}{5}}[\partial u/\partial y]_{y=0}, \end{aligned}\right\}$$

and in table 1 we show these parameters, together with the flame-sheet location, for various combustible materials which may form the surface $x > 0, y = 0$. We also remark that the value of $F(\infty)$ remains approximately constant over this range of values of $\mathscr{L}$ at about 3·5. Since it is the hot flame which acts as the primary 'sink' for the oxidant flow, the near-constancy of $F(\infty)$ is consistent with the fixed value of θ_s used in these calculations.

In figure 1 we show the distributions of velocity, temperature and the coupling

Material	$\mathscr{L}$	η_s	$F(0)$	$G''(0)$	$F''(0)$
n-octane	1·0	1·765	−2·521	0·181	1·625
Benzene	1·3	1·674	−2·313	0·217	1·753
Ethyl alcohol	2·9	1·424	−1·665	0·347	2·162
Methyl alcohol	3·8	1·351	−1·452	0·398	2·296
α-cellulose	10·0	1·151	−0·794	0·571	2·667

TABLE 1

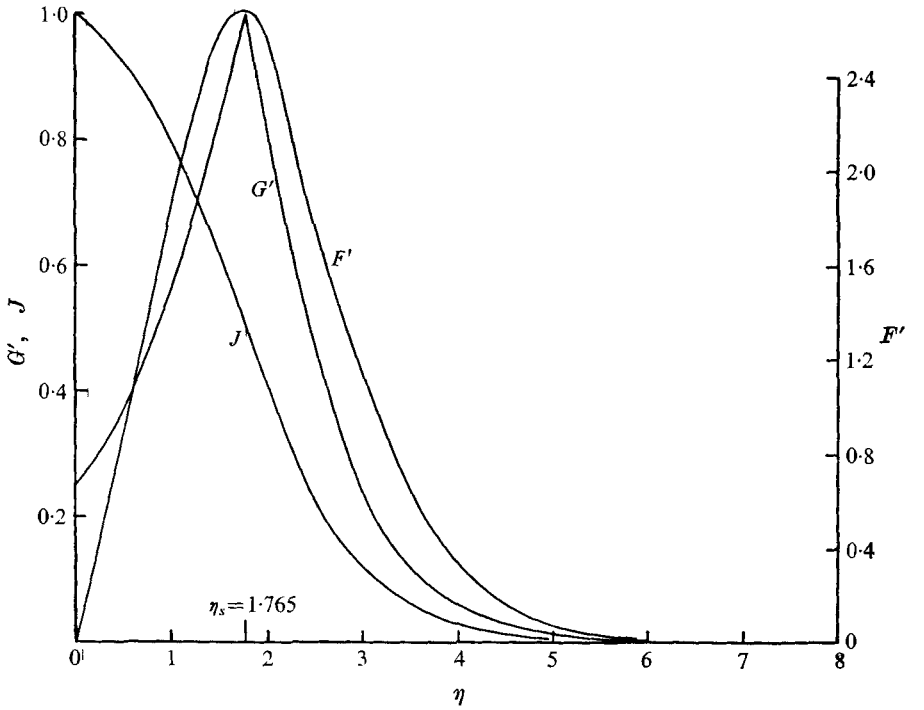

FIGURE 1. The velocity profile F', temperature G' and coupling function J for the case $\mathscr{L} = 1$.

function J in the boundary layer for the case $\mathscr{L} = 1$. These results are typical of the other values of $\mathscr{L}$; in particular we note that the velocity maximum occurs at the flame-sheet location. This is not entirely unexpected since density differences within the boundary layer are responsible for the induced pressure gradient. However it should be noted that Kim *et al.* do not find a coincidence between the velocity maximum and flame-sheet location when the plate is vertical. This is surprising since in that case buoyancy forces are directly responsible for the motion.

In figure 2 we show the flame-sheet location η_s and the transpiration rate $F(0)$ for a range of values of $\mathscr{L}$. As $\mathscr{L}$ increases we see that there is a tendency for the flame sheet to approach the fuel surface and for $\dot{m}$ to decrease. This we might expect since as $\mathscr{L}$ increases, with Δ and θ_s fixed, $\dot{m}$ must decrease for fixed η_s

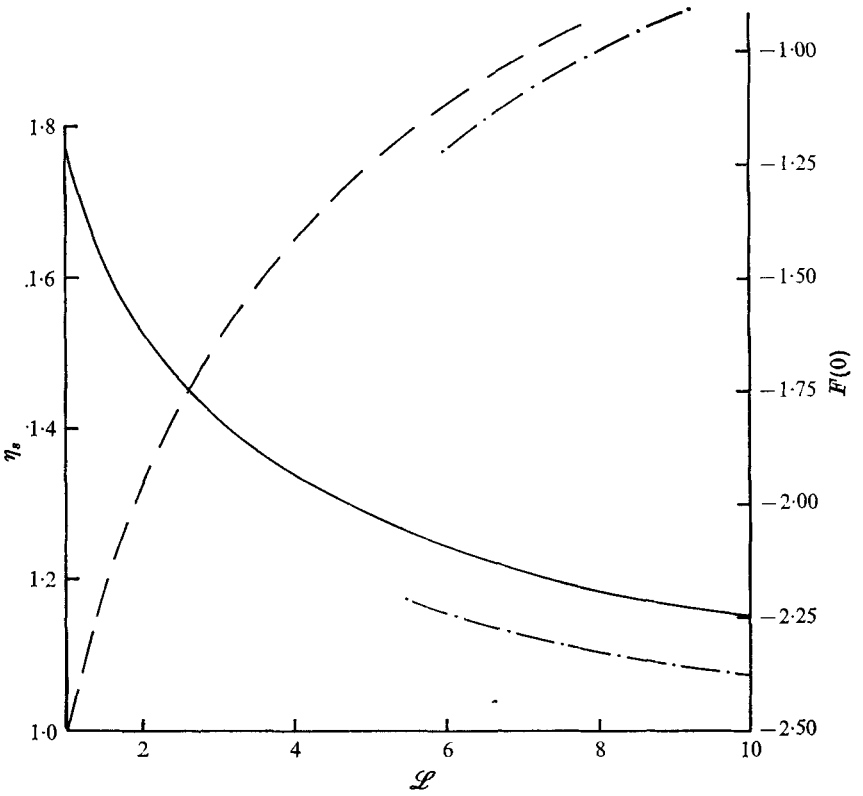

FIGURE 2. The flame-sheet location η_s (solid curve) and blowing rate $F(0)$ (dashed curve), together with their asymptotic equivalents derived from (54) and (55) for $\theta_s \gg 1$ (dot–dash curves).

[see (11)]. However any such attempt to reduce $\dot{m}$ must by itself lead to a generally thinner boundary layer and smaller value of η_s; the consequent increase in energy flux will then tend to increase $\dot{m}$ with the result that the flame will be blown away from the surface. An appropriate balance will ultimately arise which results in smaller values of η_s and $\dot{m}$ as noted. The competition between the contrary influences accounts for the relative insensitivity of η_s and $\dot{m}$ to changes in $\mathscr{L}$.

In figure 3 we show the variation of surface shear stress and heat transfer at the fuel surface for the same range of values of $\mathscr{L}$. As the flame sheet, which of course is the intense reaction zone, approaches the surface we expect the rate of surface heat transfer to increase as shown. Similarly, since the velocity maximum is always located at the flame sheet in our calculations we can expect that the surface shear stress will also increase with $\mathscr{L}$. This is confirmed by our results shown in figure 3.

Figures 4 and 5 are asymptotic equivalents for $\theta_s \gg 1$ of figures 2 and 3, derived from numerical solutions of (55). It will be recalled that in this particular asymptotic limit $\theta_s/\mathscr{L}$ is maintained as a finite quantity. In order that a comparison can be sensibly made with those calculations which have been carried

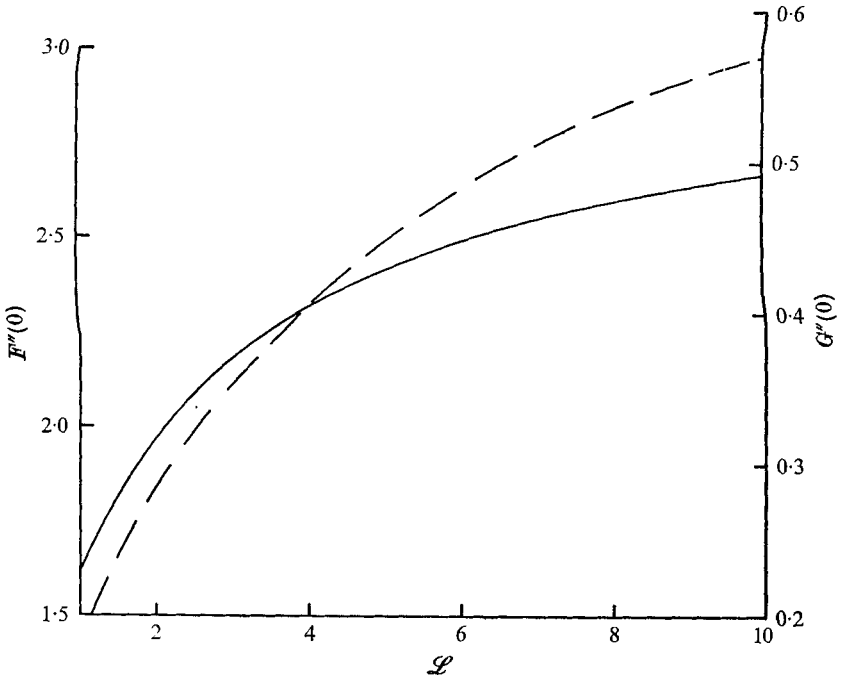

FIGURE 3. The shear-stress parameter $F''(0)$ (solid curve) and heat-transfer parameter $G''(0)$ (dashed curve).

out for $\theta_s = 6$ and finite $\mathscr{L}$ we have again chosen $\sigma = 0{\cdot}72$, $\delta = 0{\cdot}25$ and $\beta_s = 0{\cdot}5$ in our solutions of (55). The trends which we have observed for finite $\mathscr{L}$ are again present and we have included in figures 2 and 3 results inferred from our solutions for $\theta_s \gg 1$. It will be seen that the asymptotic solution gives useful information for values of θ_s which are typical in these combustion situations.

As $\mathscr{L}$ increases we have noted that the flame sheet tends to approach the fuel surface. The limit $\eta_s \to 0$ corresponds to the phenomenon of *surface combustion*. This limit can never be realized in the numerical calculations of *this* paper since we have set $\delta = 0{\cdot}25$. Thus, as $\eta_s \to 0$ we must have $\beta_s \to 1$ from the continuity of J, and from (25) we see that since Q and γ_{X_∞} will be fixed and finite on physical grounds $\Delta \to \theta_s$ or $\delta \to 1$. Although surface combustion is, then, beyond the scope of this paper we can readily discuss one particular case from the formulation of §3 and the results of I. First note that from (22*b*), with $\Delta = \theta_s$,

$$\theta_s = Q\gamma_{X_\infty} - \mathscr{L}\gamma_{X_\infty}/\gamma_{FT}; \tag{59}$$

and if (59) is now combined with (25) we have

$$\lim_{\eta_s \to 0}\left(\frac{1-\delta}{1-\beta_s}\right) = \frac{\mathscr{L}}{\theta_s}\frac{\gamma_{X_\infty}}{\gamma_{FT}}. \tag{60}$$

Now if we again adopt the limit of large flame-sheet temperature $\theta_s \gg 1$, and introduce the transformations (54), then (55) have to be solved for $\tilde{\phi}$ and $\tilde{\psi}$. Suppose that we adopt the boundary condition $\tilde{\phi}(0+) = -1$, and defer for the

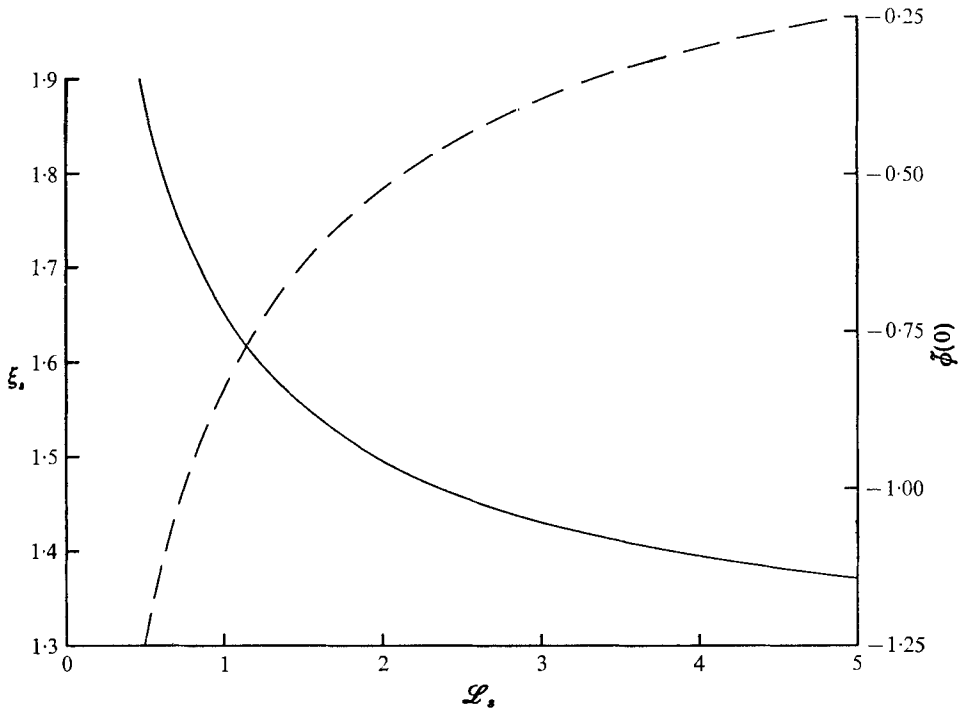

Figure 4. The asymptotic flame-sheet location ξ_s (solid curve) and the asymptotic blowing rate $\tilde{\phi}(0)$ (dashed curve) for $\theta_s \gg 1$.

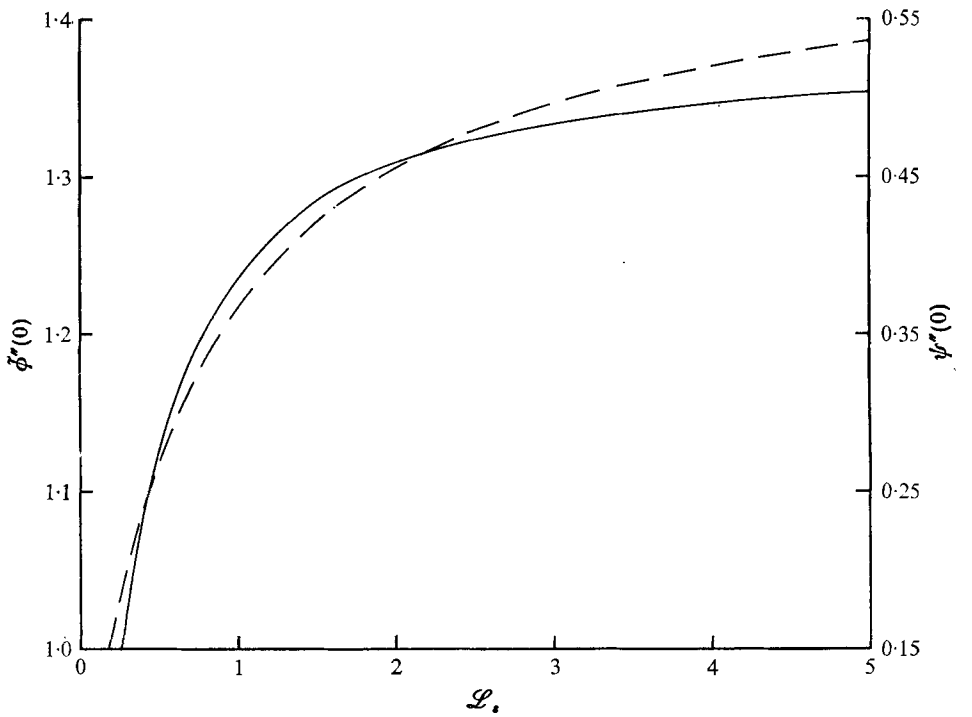

Figure 5. The asymptotic shear-stress parameter $\tilde{\phi}''(0)$ (solid curve) and heat-transfer parameter $\tilde{\psi}''(0)$ (dashed curve) for $\theta_s \gg 1$.

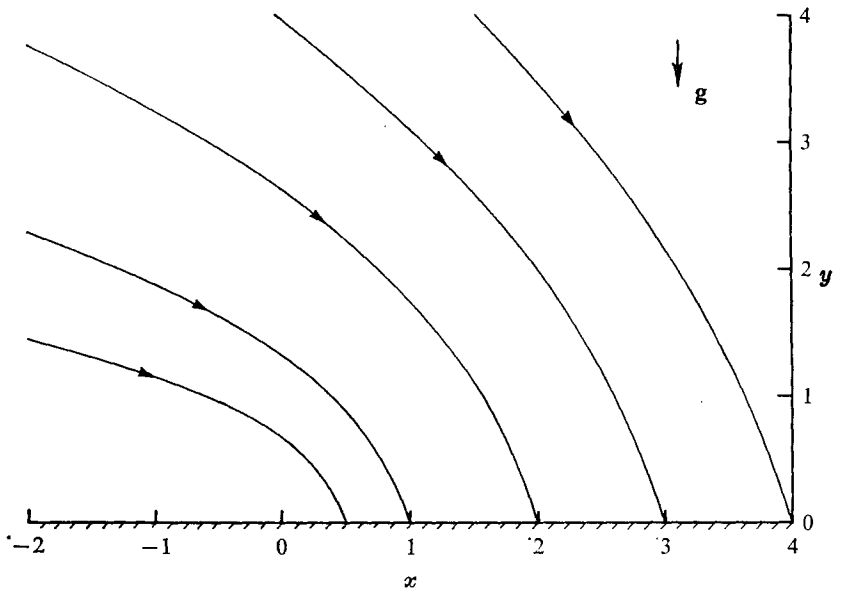

FIGURE 6. The streamlines associated with the outer flow.

moment the consequences of ignoring the condition (47a), then with the condition $\tilde{\phi}'(0+) = 0$ from (44a) and $\tilde{\psi}'(0+) = 1$ from (47b) with $\delta = 1$ together with $\tilde{\phi}'(\infty) = \tilde{\psi}(\infty) = \tilde{\psi}'(\infty) = 0$, a solution of (55) may be obtained. This problem has been studied in I, and from the results given therein for $\sigma = 0{\cdot}72$ we have

$$\tilde{\phi}''(0+) = 0{\cdot}911, \quad \tilde{\psi}''(0+) = -0{\cdot}161. \tag{61}$$

We must now examine the consequences of these results for our problem of surface combustion from a consideration of (47a). First, however, note that across the flame sheet, which now coincides with the fuel surface, we have from (50) and (60)

$$\tilde{\psi}''(0-) = \lim_{\eta_s \to 0} \left(\frac{\delta - 1}{1 - \beta_s} \right) \tilde{\psi}''(0+) = 0{\cdot}161 \mathscr{L}_s \frac{\gamma_{X_\infty}}{\gamma_{FT}}. \tag{62}$$

If we now combine (62) with (47a) we see, using (54), that surface combustion with a blowing rate $F(0) = -\theta_s^{\frac{1}{2}}$ can only be sustained under the condition $\gamma_{FT} = 0{\cdot}372\gamma_{X_\infty}$. This particular example of surface combustion gives little insight into the manner in which, for example, $\delta \to 1$ as $\eta_s \to 0$ and it is hoped to present a more detailed study of the limiting case of surface combustion, via the formulation presented in §§2 and 3, in a subsequent paper.

We consider next the flow in the region outside the boundary layer as represented by the solution (58). The streamlines associated with the outer flow, $\psi_0 =$ constant, are shown in figure 6. This demonstrates how the boundary layer entrains fluid from the surrounding ambient atmosphere to maintain the supply of oxidant for the combustion process. This outer flow models the 'fire-wind' which is observed to blow inwards across the perimeter of a fire before, if the fire is of finite extent, it develops into a vertical buoyant plume. On the

basis of their calculations, which involve no modelling of the combustion process, Smith *et al.* conclude that the fire-wind is driven by pressure forces and that the lateral inflow near a fire perimeter is of sink-like rather than boundary-layer type. As we see in figure 6 the outer flow, which we are interpreting as the fire-wind, is indeed of a sink-like character. Furthermore, as we have seen in §3, induced pressure gradients are responsible for the flow.

In the remaining section of this paper we describe a simple experiment that we have performed which helps to substantiate the theoretical work described above.

5. Experiment

A flat combustible surface was provided by clamping a number (usually two or three) of paraffin-impregnated plastic firelighters† between a pair of metal blocks. The upper surface of the metal blocks was coplanar with the flat upper surface of the firelighters and therefore simulated the situation to be found near the leading edge of the combustible interface in our theoretical model. Two parallel vertical sheets of float-glass made an open channel, with the combustible material in its floor, and provided a fair approximation to the two-dimensional geometry of the theory. The reasonable optical properties of float-glass made it possible for schlieren pictures to be taken. No attempt was made to isolate this simple apparatus from laboratory draughts, so some unsteadiness was always present in the flow which developed when combustion above the surface was fully established. Nevertheless it was possible to acquire flow and flame pictures like that exemplified in figure 7 (plate 1).

The schlieren picture shows that there is a portion of the flame sheet and its associated boundary layer which is affected by the glass channel side walls (probably accentuated by some air leakage between the glass edge and the combustible surface). Despite this imperfection we feel that the qualitative and quantitative comparisons that are illustrated in figure 7 lend substance to the theoretical predictions.

REFERENCES

CLARKE, J. F. 1975 *Prog. Aerospace Sci.* **16**, 3.

CLARKE, J. F. & RILEY, N. 1975 *Quart. J. Mech. Appl. Math.* **28**, 373.

JONES, D. R. 1973 *Quart. J. Mech. Appl. Math.* **26**, 77.

KIM, J. S., DE RIS, J. & KROESSER, F. W. 1971 *13th Symp. (Int.) on Combustion, Combustion Inst., Pittsburgh*, p. 949.

ROTEM, Z. & CLAASSEN, L. 1969 *J. Fluid Mech.* **39**, 173.

SMITH, R. K., MORTON, B. R. & LESLIE, L. M. 1975 *J. Fluid Mech.* **68**, 1.

STEWARTSON, K. 1958 *Z. angew. Math. Phys.* **9**, 276.

† 'Zip' white firelighters, Reckitt and Colman Household Division, Hull.

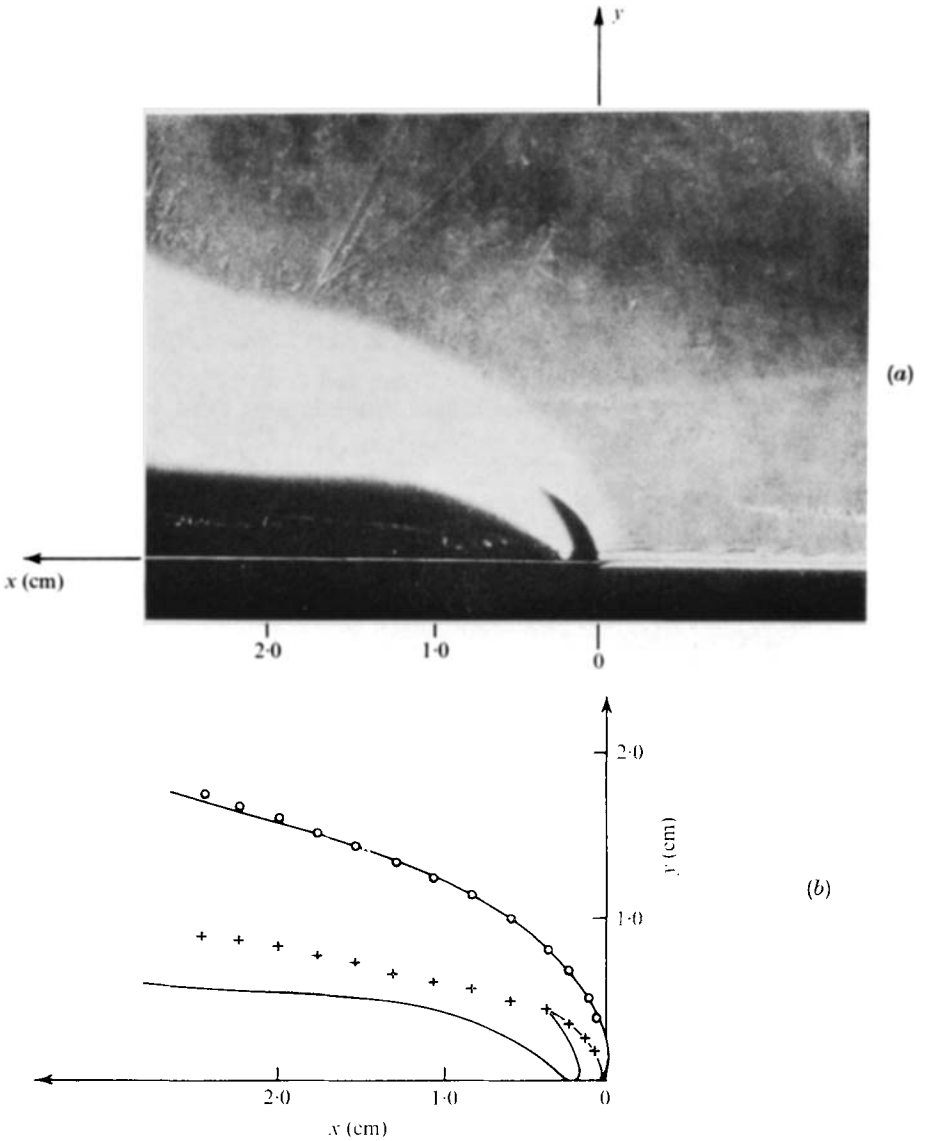

FIGURE 7. (*a*) Schlieren picture of the flow induced by the flame. The horizontal combustible surface lies along $x > 0, y = 0$. The schlieren knife-edge is horizontal; light areas have $\partial\rho/\partial y > 0$, dark areas have $\partial\rho/\partial y < 0$. The main flame sheet lies at the sharp dark/light interface (whose intersection with the x axis has been chosen as origin). The light region starting at about $x = 2$ mm indicates the presence of a secondary flame resulting from side-wall interference; it masks the main flame sheet in the region, roughly, $x > 4$ mm. (*b*) The full lines in this sketch have been traced along the dark/light interfaces on the photograph. The circles and crosses are plotted from the relation $y = Ax^{\frac{2}{5}}$ with $A = 1{\cdot}2$ and $0{\cdot}6$, respectively. If one assumes that $\theta_s = 6$ and then uses (5) and (32) it can be shown that Y is roughly $4Z$ at the flame sheet and at the outer edge of the boundary layer. It follows that the upper edge of the layer lies where η, defined in (39), has the value $\eta \equiv \eta_\infty \approx 3{\cdot}8$; the flame sheet lies at $\eta_s \approx 1{\cdot}9$. Comparison of these values with figure 1 is interesting and indicates some crude quantitative support for the theory provided that $\mathscr{L}$ is somewhat less than unity; η_∞ is less sensitive than η_s to variations in $\mathscr{L}$.